Comparison between Gadolinium-Enhanced 2D T1-Weighted Gradient-Echo and Spin-Echo Sequences in the Detection of Active Multiple Sclerosis Lesions on 3.0T MRI

Authors

F.X. Aymerich[1, 3] · C. Auger[1] · P. Alcaide-Leon[1] · D. Pareto[1] · E. Huerga[1] · J.F. Corral[1] · R. Mitjana[1] · J. Sastre-Garriga[2] · X. Montalban[2] · A. Rovira[1]

Affiliations

1. MR Unit. Department of Radiology (IDI). Hospital Universitari Vall d'Hebron. Universitat Autònoma de Barcelona, Barcelona, Spain.
2. Centre d'Esclerosi Múltiple de Catalunya (Cemcat). Department of Neurology/Neuroimmunology, Hospital Universitari Vall d'Hebron. Universitat Autònoma de Barcelona. Barcelona, Spain
3. Department of Automatic Control (ESAII), Universitat Politècnica de Catalunya – Barcelona Tech (UPC), Barcelona, Spain.

Corresponding author address:

F. Xavier Aymerich

Magnetic Resonance Unit. Department of Radiology (IDI). Hospital Universitari Vall d'Hebron.

P. Vall d'Hebron 119-129. 08035 Barcelona (Spain).

Tel.: +34934289406

Fax: +34934386059

e-mail: xavier.aymerich@idi.gencat.cat

Abstract

Objectives

To compare the sensitivity of enhancing multiple sclerosis (MS) lesions in gadolinium-enhanced 2D T1-weighted gradient-echo (GRE) and spin-echo (SE) sequences, and to assess the influence of visual conspicuity and laterality on detection of these lesions.

Methods

One-hundred MS patients underwent 3.0T brain MRI including gadolinium-enhanced 2D T1-weighted GRE and SE sequences. The two sets of contrast-enhanced scans were evaluated in random fashion by three experienced readers. Lesion conspicuity was assessed by the image contrast ratio (CR) and contrast-to-noise ratio (CNR). The intracranial region was divided into four quadrants and the impact of lesion location on detection was assessed in each slice.

Results

Six-hundred and seven gadolinium-enhancing MS lesions were identified. GRE images were more sensitive for lesion detection (0.828) than SE images (0.767). Lesions showed a higher CR in SE than in GRE images, whereas the CNR was higher in GRE than SE. Most misclassifications occurred in the right posterior quadrant.

Conclusions

The gadolinium-enhanced 2D T1-weighted GRE sequence at 3.0T MRI enables detection of enhancing MS lesions with higher sensitivity and better lesion conspicuity than 2D T1-weighted SE. Hence, we propose the use of gadolinium-enhanced GRE sequences rather than SE sequences for routine scanning of MS patients at 3.0T.

Key points

- 2D SE and GRE sequences are useful for detecting active MS lesions.
- It remains uncertain the more sensitive of these sequences at high field.
- In this study GRE sequence showed a better sensitivity and lesion conspicuity for detecting active MS lesions than SE sequence.
- We propose to use GRE sequence rather SE sequence for detecting active MS lesions at 3.0T.

Keywords

Magnetic resonance imaging · Brain · Multiple sclerosis · Contrast sensitivity · Lesion conspicuity

Abbreviations

CIS Clinically isolated syndrome

CNR Contrast-to-noise ratio

CR Contrast ratio

EDSS Kurtzke Expanded Disability Status Scale

FA Flip angle

FN False-negative

FP False-positive

GRE Gradient recalled-echo

MS Multiple sclerosis

SE Spin-echo

TP True-positive

Introduction

Gadolinium-enhanced magnetic resonance imaging (MRI) is currently the reference standard to detect active inflammatory lesions in multiple sclerosis (MS) patients [1, 2]. This technique has a pivotal diagnostic role in demonstrating dissemination in time according to the 2010 McDonald criteria [3] and is essential for assessing and predicting treatment response in clinical trials and clinical practice [4, 5]. The sensitivity of enhanced MRI to detect active lesions may vary according to the acquisition strategy used (eg, delay between injection and image acquisition, contrast dose, field strength, and frequency of MRI sampling) [1, 6, 7]. Selection of the most appropriate T1-weighted sequence after contrast injection may also influence sensitivity. Several clinical studies performed at 1.5T have shown that conventional 2D spin-echo (SE) sequences perform better than gradient recalled-echo (GRE) sequences for depicting active MS lesions after gadolinium injection [8], but it remains uncertain which of these two sequences is more sensitive for this purpose at higher field strengths [8-11].

When analyzing and comparing the sensitivity of different contrast-enhanced T1-weighted sequences to identify enhancing lesions, two concepts should be taken into account: visibility and conspicuity. Visibility usually refers to the intensity or salience of the features or properties of an object, such as the color, luminance, form, or size, whereas conspicuity refers to how well an object visually stands out from its environment [12]. In a more radiological sense, the concept of conspicuity is related to an attempt to objectively quantify radiologic observational error [13]. Conspicuity refers to how well a given feature stands out from surrounding structures, and it can be defined as the ratio between the lesion contrast and the complexity of the surroundings [13, 14]. Other factors such as visual laterality, which is based on lateral masking, a phenomenon in which the peripheral perception of a visual target is impaired when

distractors are present in the adjacent surroundings [15], can also influence lesion detection.

The aims of this study were to compare the sensitivity of active MS lesion detection in gadolinium-enhanced T1-weighted GRE and SE sequences, determine the influence of visual conspicuity and laterality on detection of these lesions, and investigate whether the topographic distribution of the lesions has an impact on their detection. The hypothesis was that the use of GRE sequences would provide better lesion detection than SE sequences at 3.0T, as the latter sequence may result in ghosting artifacts due to of vessel pulsation, leading to an increase in background noise.

Materials and Methods

Patients

Patients 18 to 50 years of age with a CIS suggestive of CNS demyelination unattributable to other diseases and patients with a diagnosis of relapsing MS based on the McDonald 2010 criteria [3] showing at least 2 brain T2 lesions of the type seen in MS were eligible for inclusion in the study. CIS patients were scanned within the first 3 months after symptoms onset as part of their initial routine assessment, and relapsing MS patients were scanned because of suspected disease activity.

The exclusion criteria were pregnant or nursing women, patients having a pacemaker or any other factor that would preclude proximity to a strong magnetic field, those with severe claustrophobia or a known allergy to gadolinium compounds, administration of steroids within the 30 days before MRI scanning, and known severe renal function impairment.

The study included 100 consecutive patients (73 women; overall mean age, 35.8 years; range [23, 50] years), with a median Kurtzke Expanded Disability Status Scale (EDSS)

score of 3 (range, [0, 8]). Twenty-six patients had a CIS, and 74 a diagnosis of relapsing-remitting MS [3, 16]. The study was approved by the Ethics Committee of our institution and written informed consent was obtained from all patients for participation.

MRI acquisition

All patients were examined on a 3.0T MRI scanner (Magentom Trio, Siemens, Erlangen, Germany) using a 12-channel head coil. The MRI protocol followed the standard of practice in our institution, and included the following sequences:

1) Transverse proton density and T2-weighted fast spin-echo (repetition time [TR], 2500 ms; echo time [TE], 16-91 ms; voxel size, 0.78x0.78x3.0 mm^3; flip angle [FA], 150º; acquisitions [Acq], 2; acquisition time [TA], 4:52 min).

2) Transverse fast T2-FLAIR (TR, 9000 ms; TE, 100 ms; inversion time [TI], 2500ms; FA, 120º; voxel size, 1.0x1.0x3.0 mm^3; Acq, 1; TA, 4:14 min).

3) Post-contrast sequences: 15 minutes after injection of a double dose of gadobutrol (0.2 mmol/kg), a T1-weighted GRE sequence was acquired (TR, 297 ms; TE, 2.46 ms; FA, 70º; voxel size, 0.78x0.78x3.0 mm^3; Acq, 3; TA, 3:50 min). Just before GRE sequence acquisition in half the patients and just after in the other half, an SE sequence was acquired (TR, 480 ms; TE, 20 ms; FA, 90º; voxel size, 0.78x0.78x3.0 mm^3; Acq, 1; TA, 5:31 min). Both sequences were acquired without activating acceleration in the acquisition.

All sequences were acquired using 3-mm-thickness contiguous slices covering the whole brain. In our center, we routinely use a double dose of gadobutrol (0.2 mmol/kg) for evaluating MS patients. Our experience (unpublished data) and data from the literature [17, 18] have shown that this strategy increases the sensitivity of MRI for

detecting gadolinium-enhancing brain lesions by decreasing the T1 relaxation time effect.

Image analysis

In each set of T1-weighted sequences, three readers (R.M., E.H. and J.F.C.), with more than 10 years' experience analyzing MR images in clinical studies and clinical trials related to MS, identified the enhanced MS lesions independently, separately, and in randomized order. Readers were blinded to any additional information other than the contrast-enhanced T1-weighted sequence they were interpreting.

The reference standard for the enhanced MS lesions was defined by consensus between two of the authors (P.A. and A.R.), with 2 and more than 20 years of experience. These specialists did not participate in the blinded reading. They jointly reviewed the MR imaging datasets and had access to the clinical data, the radiological report, and all the MR sequences performed. An enhanced MS lesion was defined as a focal enhancement on post-contrast images, with a large enough size to differentiate it from its local background, involving gray or white matter and associated with a parenchymal hyperintensity on T2-FLAIR or T2-weighted images. Each MS lesion identified based on these criteria computed as one lesion in the reference standard, regardless of whether it was better or more poorly perceived in the GRE or the SE images. One of the authors (P.A.) then delineated each lesion in both the SE and GRE images using the semiautomated tool included in Jim 5.0 (Xinapse Systems Ltd, Essex, UK), which additionally provided the lesion volume. Qualitative information was also recorded on the location of the lesions (periventricular, subcortical, juxtacortical, or infratentorial), the contrast uptake pattern (nodular, ring, open-ring, or heterogeneous), and the lesion differentiability, defined as the ease with which a lesion could be identified in an image, graded on a 5-point scale: very poor, poor, fair, good, or excellent.

The lesions identified by the three readers were then compared with the reference standard to determine the number of true-positive (TP), false-negative (FN) and false-positive (FP) identifications. The sensitivity values were calculated as follows: S=TP/(TP+FN). Using an in-house-developed program, identifications corresponding to TPs and FNs were matched with the lesion delineation defined in the reference standard. Lastly, detections corresponding to FPs were newly delineated.

To obtain quantitative measurements related to the visual conspicuity of the lesions, the contrast ratio (CR) and contrast-to-noise ratio (CNR) were evaluated in each of the lesion detection groups (TP, FP, FN). The contrast ratio between the MS lesion and its background was calculated using the formula CR=(SI lesion - SI background)/SI background, and the contrast-to-noise ratio was calculated as CNR=(SI lesion - SI background)/SD noise, where SI represents the signal intensity of a region and SD noise the standard deviation of the noise measured in the background of the image. Two background 3-pixel and 5-pixel-width areas surrounding the lesions were selected, and 4 quantitative measures to evaluate visual conspicuity were computed: CR3, CR5, CNR3, and CNR5. Finally, the effect of visual laterality was evaluated in each slice by first tracing a horizontal and vertical line crossing at the brain center and dividing the brain into four quadrants to establish the topographic distribution of lesions. The number of lesions, and the number of TP, FN, and FP detections were then computed in each quadrant.

Statistical analysis

Statistical analyses were performed using SPSS v13.0 software (IBM Corp., USA). Statistical differences in lesion counting by each reader were compared per patient using the Wilcoxon signed-rank test. In addition, the sensitivity values for detecting lesions in

both sequences were calculated for each reader and for the overall group. To evaluate the performance of the conspicuity indexes between the lesion detection groups, we used analysis of variance (ANOVA), with Dunnett's T3 test as a post-hoc test to consider non-homogeneity of the variances in the groups. P-values of less than 0.05 were considered statistically significant. Finally, we used conspicuity measurements to determine whether the lesion detection groups could be differentiated by their visual properties. The conspicuity measurements for each lesion detection group were classified in clusters. We then calculated the separability of the conspicuity measurements between detection groups using a measure of distance between clusters. The distance between two clusters was computed as dAB=|mA-mB|/(SDA+SDB), where mI and SDI were, respectively, the mean and standard deviation of the values of a conspicuity index for a cluster I={A, B}. According to this metric, the higher the value the greater the distance between two clusters, and consequently, the better the separability between the lesion detection groups based on visual conspicuity.

Results

Reference standard

Following evaluation of all the available MR sequences, 607 gadolinium-enhancing MS lesions were found in 100 patients (mean number of lesions per patient, 6.07; SD, 13.10; range, [0, 107]; patients without gadolinium-enhancing lesions, 38; median of lesions in patients with at least one gadolinium-enhancing lesion, 4), with a mean volume of 119.4 mm^3 in SE images (range, [1.1, 3158.6]) and 120.5 mm^3 in GRE images (range, [1.8, 3158.6]). The high percentage of patients with at least one gadolinium-enhancing lesion, and the high number of gadolinium-enhancing lesions could be explained by the fact that all patients had recent clinical activity.

By anatomical location, 274 lesions (45.14%) were subcortical, 165 (27.18%) juxtacortical, 105 (17.30%) periventricular, and 63 (10.38%) infratentorial. Most of the lesions found (527, 86.82%) showed a nodular pattern of contrast uptake, 13 (2.14%) showed a ring pattern, 34 (5.60%) an open-ring, and 33 (5.43%) were heterogeneous. In SE images, differentiability was rated as excellent in 251 lesions, good in 114, fair in 94, poor in 79, and very poor in 69, whereas in GRE images, differentiability was considered excellent in 217 lesions, good in 142, fair in 91, poor in 70, and very poor in 87.

Effect of the order in which sequences were acquired

In half the patients SE sequences were acquired before GRE (SE-GRE) and in the other half GRE sequences were acquired before SE (GRE-SE). According to the reference standard, the distribution of lesions was balanced: 49.9% were detected in patients undergoing SE sequences first and 50.1% in those undergoing GRE first. There were only small differences between TPs, FNs, FPs, and sensitivity according to the order in which sequences were acquired (Table 1). Furthermore, the sensitivity of each sequence increased in a similar manner when it was acquired in second place. Hence, we consider that there was no relevant effect of the order in which sequences were acquired on their performance.

Agreement between readers and the reference standard

Figure 1 shows an example of TPs, FNs, and FPs marked by readers using the two T1-weighted sequences. On qualitative assessment, TPs varied considerably in size and shape, whereas FNs and FPs were usually smaller lesions. The total number of detections, the number of TPs, FPs, and FNs, the sensitivity values for each reader, and

the mean sensitivity values for the three readers are summarized in Table 2. GRE images had a higher number of TP detections; consequently the number of FNs was lower and the sensitivity higher (GRE, 0.828; SE, 0.767). The number of FP detections was very similar in the two sequences (SE, 2.75%; GRE, 2.69%). On patient-wise analysis, differences in the number of TPs between SE and GRE images were significant between all the readers (p=0.018, 0.013, <0.001, respectively) and differences in the number of FNs were significant between 2 of the 3 readers (p=0.119, 0.041, 0.005, respectively). There were no significant differences between the readers for the number of FPs (p=0.702, 0.501, 0.609, respectively).

The majority of reference standard markings were rated as having fair to excellent differentiability in both SE and GRE sequences, with somewhat better differentiability in SE images, inferred from a greater number of lesions classified as excellent in this sequence (Table 3). However, there were fewer FNs in GRE images than SE images. Moreover, the FNs in GRE images were mainly classified as having very poor differentiability, whereas FNs in SE images were distributed from very poor to fair differentiability.

Visual conspicuity and laterality

The results obtained using the conspicuity indices are shown in Table 4. Overall, the CR values were higher for SE images, whereas CNR values were higher for GRE images. Statistically significant differences in TP, FN, and FP detection were observed across all four indices (p-value<0.001). To select the sequence with better performance, we also analyzed a distance measure whose values are shown in Table 5. CNR3 measurements showed the highest distance between TP and FN in GRE images (dTPFN=0.612), and between TP and FP in SE images (dTPFP=0.550).

Finally, the analysis of visual laterality showed that FNs were mainly located in the posterior quadrants in both GRE and SE images (Figure 2). Although there were no large differences between the two sides, the right posterior quadrant (quadrant 2 in the Figure), was the region in which the largest number of FN readings occurred: 21.23% of lesions identified in this quadrant using the GRE sequence and 25.68% using the SE sequence.

Discussion

The results of this study show that the sensitivity for detecting gadolinium-enhancing lesions on a 3.0T system was higher with the use of 2D GRE sequences than with 2D SE sequences. To date, most clinical studies and trials in MS have been carried out using 1.5T magnets [19-21]. There is much less available data related to the use of 3.0T magnets, which are becoming increasingly more common in the clinical setting.

As relates to MS, 3.0T systems offer some advantages over lower field strengths, such as higher detection rates for T2 and gadolinium-enhancing brain lesions [22-24], an important capability for diagnosing and monitoring MS patients. Some studies performed at 1.5T have shown that conventional 2D SE sequences are apparently better than GRE sequences for depicting gadolinium-enhancing lesions [8], but the most appropriate T1-weighted sequence for detecting these lesions at 3.0T is still a matter of debate.

The findings from a previous study comparing 2D SE and GRE sequences for brain imaging at 3.0T (although not specifically focused on MS) suggested that GRE may be more sensitive for detecting contrast-enhancing lesions [25]. This is consistent with our results in MS lesions, and GRE has the additional advantage of a shorter acquisition time.

Another issue to take into account is the readers' identification errors (prevalence of FNs versus FPs) when interpreting the two sequences. In the present study, the number of FPs did not reach 20% of the number of FNs, and the number of FNs was about 25% of the total number of lesions. SE images showed poorer performance than GRE in terms of FN detection.

The qualitative approach to identify lesions seemed to provide somewhat better results when SE sequences were analyzed: a larger number of lesions were rated as excellent in this sequence according to the reference standard. Furthermore, the subjective differentiability of lesions defined in the reference standard seemed to be related to the CR. The findings on quantitative analysis, however, seem to contradict these qualitative results: GRE showed higher sensitivity for lesion detection and a higher CNR than SE. This contradiction may have arisen because the subjective approach may be more related to the visibility of lesions than to their conspicuity. Analysis of the CNR, which better assesses the complexity of the surroundings around the lesions than the CR by taking into account factors such as image noise, provided results that better matched the sensitivity values found.

To investigate the complexity of the tissue surrounding the lesions, we introduced 2 widths of the surrounding area for the lesion background. Nonetheless, the extension of this area did not seem relevant, as the results obtained for the 2 widths were very similar.

In the study of the effect of visual laterality on lesion detection, we found a higher probability of FN detection in lesions located in the posterior quadrants than in those with frontal locations. Hence, detection of lesions in areas mainly located in these quadrants, such as the infratentorial region, may be more complex.

Our study has some limitations. First, the GRE and SE sequences were not acquired at the same time after contrast injection. To compensate for this fact, SE images were acquired just before acquisition of GRE images in half the patients, and just after in the other half. However, our analysis of this factor showed that the order in which sequences were acquired seemed to have no effect on the results obtained. Second, the study only investigated 2D sequences, as 2D sequences remain the standard performed in many clinical trials and research studies [26]. 3D sequences represent a potentially valuable alternative because a large number of thin contiguous sections can be acquired in a relatively short imaging time, thus providing high-resolution coverage of the complete volume of interest and a data set that can be reformatted to obtain high-quality images in any plane [27]. Recent studies have shown that at 3T, 3D GRE or 3D fast SE sequences provide higher detection rates for gadolinium-enhancing MS lesions, especially smaller ones, than standard 2D SE, and better suppress artifacts related to vascular pulsation [10, 11]. However, these data were published after the time when the present study was designed. Lastly, it was not possible to define a strict gold standard to determine the TP, FN, and FP rates, as subjective measurements are never absolutely free from error. Instead, we used a comparator reference standard established on consensus. It is important to stress that a lesion included in the reference standard was the comparator for both sequences, regardless of whether it had been better or more poorly perceived in each sequence; hence, the comparison can be considered valid.

In conclusion, this study shows that the contrast-enhanced 2D T1-weighted GRE sequence on 3.0T MRI enables detection of enhancing MS lesions with higher sensitivity than the 2D T1-weighted SE sequence and provides better lesion conspicuity. Because of the important role of MRI in diagnosing MS and in assessing and predicting treatment response, these results may be relevant to clinical practice. Therefore, we

propose using contrast-enhanced GRE sequences instead of SE sequences for routine scanning of MS patients at 3.0T.

Acknowledgements

The authors thank Celine Cavallo for English language support, and Isidre Rivero and Ignasi Ferrer for their help in post-processing.

References

1. Filippi M, Rocca M (2011) MR imaging of multiple sclerosis. Radiology 259:659-681.

2. Bakshi R1, Thompson AJ, Rocca MA et al (2008) MRI in multiple sclerosis: current status and future prospects. Lancet Neurol. 7:615-625.

3. Polman CH, Reingold SC, Banwell B et al (2011) Diagnostic criteria for multiple sclerosis: 2010 revisions to the McDonald criteria. Ann Neurol 69:292-302

4. Sormani MP, Bruzzi P (2013) MRI lesions as a surrogate for relapses in multiple sclerosis: a meta-analysis of randomised trials. Lancet Neurol. 12:669-676.

5. Río J, Castilló J, Rovira A et al (2009) Measures in the first year of therapy predict the response to interferon β in MS. Multiple Sclerosis 15:848-853.

6. Rovira A, León A (2008). MR in the diagnosis and monitoring of multiple sclerosis: An overview. Eur J Radiol 67:409–414.

7. Filippi M (2000). Enhanced magnetic resonance imaging in multiple sclerosis. Multiple Sclerosis 6:320-326.

8. Runge VM, Patel MC, Baumann SS et al (2006) T1-weighted imaging of the brain at 3 Tesla using a 2-dimensional spoiled gradient echo technique. Invest Radiol 41:68-75.

9. Fischbach F, Bruhn H, Pech M et al (2005). Efficacy of contrast medium use for neuroimaging at 3.0 T: utility of IR-FSE compared to other T1-weighted pulse sequences. J Comput Assist Tomogr 29:499-505.

10. Hodel J, Outteryck O, Ryo E et al (2014) Accuracy of postcontrast 3D turbo spin-echo MR sequence for the detection of enhanced inflammatory lesions in patients with multiple sclerosis. AJNR Am J Neuroradiol 35:519-523.

11. Crombé A, Saranathan M, Ruet A et al (2015) MS Lesions are better detected with 3D T1 gradient-echo than with 2D T1 spin-echo gadolinium-enhanced imaging at 3T. AJNR Am J Neuroradiol 36:501-507.

12. Wertheim AH (2010) Visual conspicuity: a new simple standard, its reliability, validity and applicability. Ergonomics 53:421-442.

13. Kundel HL, Revesz G (1976) Lesion conspicuity, structured noise, and film reader error. AJR Am J Roentgenol 126:1233-1238.

14. Revesz G (1985) Conspicuity and uncertainty in the radiographic detection of lesions. Radiology 154:625-628.

15. Wertheim AH, Hooge ITC, Krikke K, Johnson A (2006) How important is lateral masking in visual search?. Exp Brain Res 170:387-402.

16. Lublin FD, Reingold SC, Cohen JA et al (2014) Defining the clinical course of multiple sclerosis. Neurology 83:1-9.

17 Filippi (2000) M. Enhanced magnetic resonance imaging in multiple sclerosis. Multiple Sclerosis 6:320-326

18 Rovira A (2009) Gadolinium-enhanced magnetic resonance imaging in multiple sclerosis. EJHP Practice 15:33-35.

19. Frohman EM, Cutter G, Remington G et al (2010) A randomized, blinded, parallel-group, pilot trial of mycophenolate mofetil (CellCept) compared with interferon beta 1-a (Avonex) in patients with relapsing-remitting multiple sclerosis. Therapeutic Advances in Neurological Disorders 3:15-28.

20. Gómez-Moreno M, Díaz-Sánchez M, Ramos-González A (2012) Application of the 2010 McDonald criteria for the diagnosis of multiple sclerosis in a Spanish cohort of patients with clinically isolated syndromes. Multiple Sclerosis Journal 18:39-44.

21. Swanton JK, Rovira A, Tintoré M et al (2007) MRI criteria for multiple sclerosis in patients presenting with clinically isolated syndromes: a multicentre retrospective study. Lancet Neurol 6:677-686.

22. Sicotte NL, Voskuhl RR, Bouvier S, Klutch R, Cohen MS, Mazziotta JC (2003) Comparison of multiple sclerosis lesions at 1.5 and 3.0 Tesla. Invest Radiol 38:423-427.

23. Wattjes MP, Lutterbey GG, Harzheim M, et al (2006) Higher sensitivity in the detection of inflammatory brain lesions in patients with clinically isolated syndromes suggestive of multiple sclerosis using high field MRI: an intraindividual comparison of 1.5 T with 3.0 T. Eur Radiol 16:2067-2073.

24. Wattjes MP, Harzheim M, Kuhl CK, et al (2006) Does high-field MR imaging have an influence on the classification of patients with clinically isolated syndromes according to current diagnostic MR imaging criteria for multiple sclerosis?. AJNR Am J Neuroradiol 27:1794-1798.

25. Stehling C, Niederstadt T, Krämer S et al (2005) [Comparison of a T1-weighted inversion-recovery-, gradient-echo- and spin-echo sequence for imaging of the brain at 3.0 Tesla]. Rofo 177:536-542.

26. Lövblad KO, Anzalone N, Dörfler et al (2010) MR image in multiple sclerosis: Review and recommendations for current practice. AJNR Am J Neuroradiol 31: 983-989.

27. Mugler JP 3rd, Brookeman JR (1993) Theoretical analysis of gadopentetate dimeglumine enhancement in T1-weighted imaging of the brain: comparison of two-dimensional spin-echo and three-dimensional gradient-echo sequences. J Magn Reson Imaging 3:761-769.

Tables

Table 1. Effect of the order in which sequences were acquired on the agreement between readers' assessment and the reference standard

		SE-GRE	*GRE-SE*
SE	**TP**	227.67	237.67
	FP	8.0	8.67
	FN	75.33	66.33
	Sensitivity	0.751	0.782
GRE	**TP**	255.67	250.0
	FP	8.33	8.0
	FN	48.33	57.0
	Sensitivity	0.841	0.814

GRE, gradient-echo; SE, spin-echo; TP, true positives; FP, false positives; FN, false negatives

Table 2. Agreement between the readers' assessment and the reference standard

		Reader 1	*Reader 2*	*Reader 3*	*Mean*
SE	**TP**	481 (79.24)	475 (78.25)	440 (72.49)	**465.33 (76.66)**
	FP	17 (2.80)	24 (3.95)	9 (1.48)	**16.67 (2.75)**
	FN	126 (20.76)	132 (21.75)	167 (27.51)	**141.67 (23.34)**
	Total	624	631	616	
	Sensitivity	0.792	0.783	0.725	**0.767**
GRE	**TP**	508 (83.6)	499 (82.21)	498 (82.04)	**501.67 (82.65)**
	FP	17 (2.80)	18 (2.97)	14 (2.31)	**16.33 (2.69)**
	FN	99 (16.31)	108 (17.79)	109 (17.96)	**105.33 (17.35)**
	Total	624	625	621	
	Sensitivity	0.838	0.823	0.822	**0.828**

GRE, gradient-echo; SE, spin-echo; TP, true positives; FP, false positives; FN, false negatives

*Values between parentheses represent the percentage of the total number of lesions identified in the reference standard.

Table 3. Differentiability of the lesions detected

			Very poor	*Poor*	*Fair*	*Good*	*Excellent*
SE	**Readers**	**FN**	51.33 (8.46)	42.33 (6.97)	30 (4.94)	11 (1.81)	7 (1.15)
		TP	17.67 (2.91)	36.67 (6.04)	64 (10.54)	103 (16.97)	244 (40.20)
		FP	3 (0.49)	5.33 (0.88)	7 (1.15)	0.67 (0.11)	0.67 (0.11)
	RS		69 (11.37)	79 (13.01)	94 (15.49)	114 (18.78)	251 (41.35)
GRE	**Readers**	**FN**	56.33 (9.28)	21.67 (3.57)	18.33 (3.02)	6 (0.99)	4 (0.66)
		TP	30.67 (5.05)	48.33 (7.96)	72.67 (11.97)	137 (22.57)	213 (35.09)
		FP	6 (0.99)	4.67 (0.77)	5.33 (0.88)	1.67 (0.28)	0.33 (0.05)
	RS		87 (14.33)	70 (11.53)	91 (14.99)	142 (23.39)	217 (35.75)

GRE, gradient-echo; SE, spin-echo; TP, true positives; FP, false positives; FN, false negatives; RS, reference standard

*Values between parentheses represent the percentages of the total number of lesions identified in the reference standard

Table 4. Visual conspicuity indices of the lesions detected

		CR3	*CR5*	*CNR3*	*CNR5*
SE	**FN**	0.20	0.22	13.69	14.79
	TP	0.37	0.40	27.26	28.54
	FP	0.25	0.29	14.85	16.32
GRE	**FN**	0.11	0.13	17.02	19.35
	TP	0.23	0.26	37.76	40.61
	FP	0.16	0.18	20.71	23.42

CR3, contrast ratio with 3-pixel background; CR5, contrast ratio with 5-pixel background; CNR3, contrast-to-noise ratio with 3-pixel background; CR5, contrast-to-noise ratio with 5-pixel background; GRE, gradient-echo; SE, spin-echo; TP, true positives; FP, false positives; FN, false negatives

Table 5. Distance between detections in SE and GRE images

		SE			*GRE*		
		FN	***TP***	***FP***	***FN***	***TP***	***FP***
CR3	**FN**	0.0	0.589	0.200	0.0	0.592	0.220
	TP	0.589	0.0	0.351	0.592	0.0	0.318
	FP	0.200	0.351	0.0	0.220	0.318	0.0
CR5	**FN**	0.0	0.585	0.232	0.0	0.582	0.075
	TP	0.585	0.0	0.296	0.573	0.0	0.280
	FP	0.232	0.296	0.0	0.234	0.280	0.0
CNR3	**FN**	0.0	0.582	0.075	0.0	0.612	0.127
	TP	0.582	0.0	0.550	0.612	0.0	0.450
	FP	0.075	0.550	0.0	0.127	0.450	0.0
CNR5	**FN**	0.0	0.572	0.093	0.0	0.600	0.131
	TP	0.572	0.0	0.524	0.600	0.0	0.431
	FP	0.093	0.524	0.0	0.131	0.431	0.0

CR3, contrast ratio with 3-pixel background; CR5, contrast ratio with 5-pixel background; CNR3, contrast-to-noise ratio with 3-pixel background; CR5, contrast-to-noise ratio with 5-pixel background; GRE, gradient-echo; SE, spin-echo; TP, true positives; FP, false positives; FN, false negatives

Figures

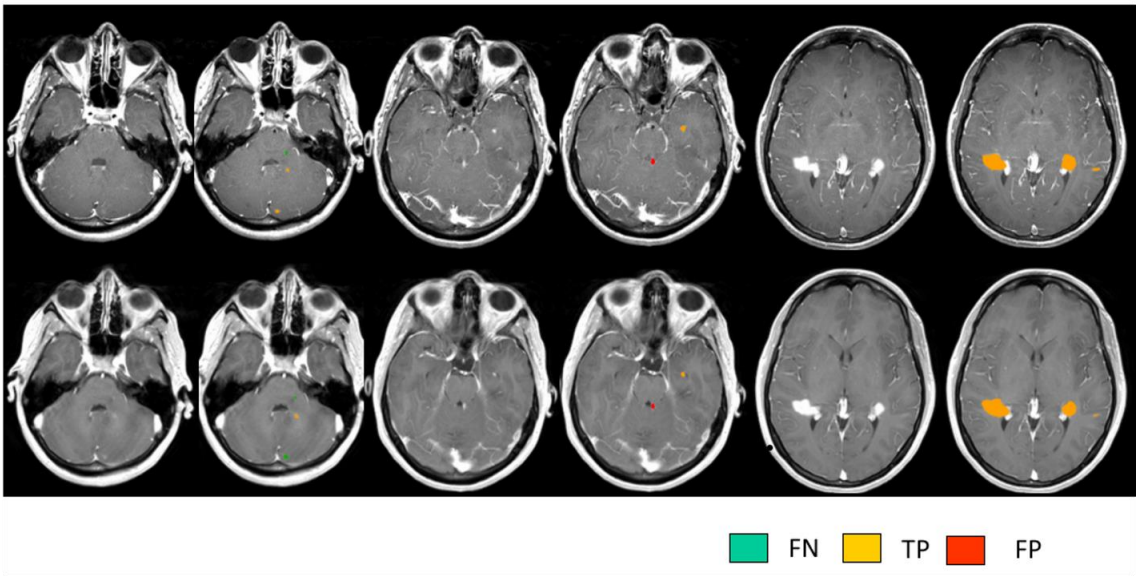

Figure 1. Example of agreement between a reader and the reference standard for three slices. Spin-echo and gradient-recalled echo images are depicted in the top and bottom row, respectively. Each slice is shown in two columns. The left one shows the original images, and the right one an image with the type of detection in a color overlay (green, false negatives [FN], orange, true positives [TP], and red, false positives [FP]).

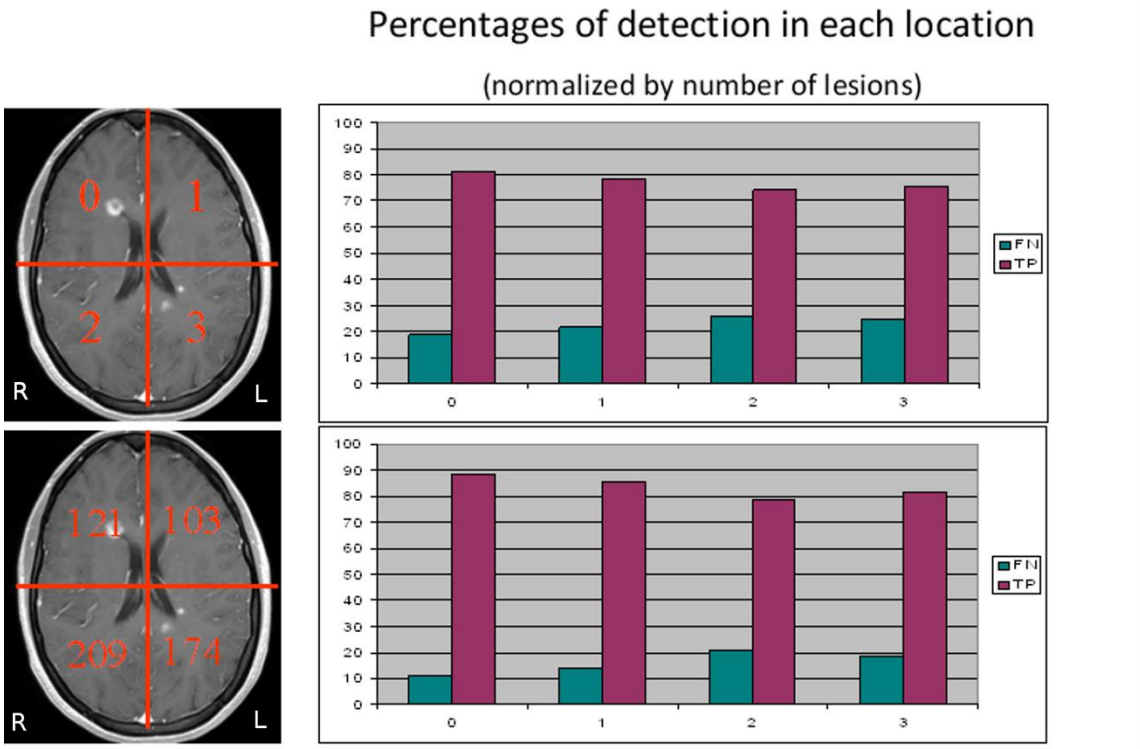

Figure 2. Effect of visual laterality on lesion detection. The left images show division of a representative image into four quadrants, numbered in red from 0 to 3 in the top image overlay. The number of lesions in the reference standard contained in each quadrant is shown in red overlay in the bottom image. The plots show the percentages of detection in each location, defined by the numbers associated with each quadrant, for spin-echo (top) and gradient recalled-echo (bottom) images. These plots represent the percentages normalized to the total number of false negative (FN) and true positive (TP) lesions per location.